

A Tri-modal 2024 Al -B₄C composites with super-high strength and ductility: Effect of coarse-grained aluminum fraction on mechanical behavior

Alireza Abdollahi* and Ali Alizadeh

Faculty of Materials & Manufacturing Processes, Malek-e-Ashtar University of Technology, Tehran, Iran.

Received 5 May 2014; Accepted 24 November 2014

* Corresponding author: *alirezaabdollahi1366@gmail.com*

Abstract

In this study, ultrafine grained 2024 Al alloy based B₄C particles reinforced composite was produced by mechanical milling and hot extrusion. Mechanical milling was used to synthesize the nanostructured Al2024 in attrition mill under argon atmosphere up to 50h. A similar process was used to produce Al2024-5%wt. B₄C composite powder. To produce trimodal composites, milled powders were combined with coarse grained aluminum in 30 and 50 wt% and then were exposed to hot extrusion at 570°C. The microstructure of hot extruded samples were studied by optical microscope, Transmission electron microscope (TEM) and scanning electron microscope (SEM) equipped with EDS spectroscopy. The mechanical properties of samples were compared by using tensile, compression and hardness tests. The results showed that the strength, after 50 h milling and addition of 5wt% B₄C, increased from 340 to 582 MPa and the hardness increased from 87 HBN to 173 HBN, but the elongation decreased from 14 to 0.5%. By adding the coarse-grained aluminum powder, the strength and hardness decreased slightly, but the increases in return. Ductility increase is the result of increase in dislocation movements and strength increase is the result of restriction in plastic deformation by nanostructured regions. Furthermore, the strength and hardness of trimodal composites were higher, but their ductility was lower.

Keywords: *aluminum matrix composites, ultra-fine grained materials, trimodal composites, carbides.*

1. Introduction

In the recent years, nanostructured, or ultrafine grained metal matrix composites are used increasingly in industry and technology areas, because of their excellent properties, such low density, high strength and good hardness [1-3].

Two basic approaches have been used to

fabricate bulk nanostructured materials. In the first approach, nanostructured powders are produced and then consolidated, while the second approach reduces the microstructure of bulk sample to the nanostructured scale by means of severe plastic deformation (SPD)

processes, such as equal channel angular pressing (ECAP), or high-pressure torsion [1,4]. In the first method, the mechanical milling process is used for nanostructured metal powder production.

Although nanostructured metal based composites have high strength and low density, but one of the main disadvantages of these composites is their very low ductility, compared to coarse-grained metal matrix composites [2, 5]. Further, the compressibility of these powders is very low [6]. The low ductility of these structures is attributed to restriction of dislocation movement [7].

The recent studies show that a uniform distribution of micro-sized particles in nanostructured metal matrix, leads to increase in ductility without any remarkable decrease in strength. This study has been conducted on various alloys, such as, Al5083 and copper. In this method, by mixing different percentage of nanostructured powder (milled powder) and coarse-grained powder the desired strength and ductility could be achieved. It has been demonstrated by the authors previous work that nanocrystalline Al with B₄C fractured in the elastic deformation region, regardless of its high strength [8]. The idea behind the present work, ignited by the successful work by Witkin *et al.* [4,5,7] and Han *et al.* [9,10], was to introduce some coarse-grained Al into the nanocrystalline Al reinforced with B₄C particles to create a material with greatly improved strength and acceptable ductility.

The bimodal metals/alloys were first reported by Tellkamp *et al.* [11]. Han *et al.* [9] Prepared bimodal 5083 Al alloy with high strength and good ductility through cryomilling and hot extrusion. In another research, they produced Al5083-15% unmilled Al, Al5083-30% unmilled Al and Al5083-50% unmilled Al via through cryomilling of nanostructured 5083 Al powders, selectively mixing the nanostructured powders with coarse-grained powders, consolidation of the mixture by cold isostatic pressing (CIP), and hot extrusion. An enhanced tensile elongation was observed in the bimodal alloys [10].

Hofmeister *et al.* [12] have studied the strength and ductility of Al-B₄C trimodal composites consisting of a nanostructured Al phase (NC Al), B₄C particulates, and a coarse-

grained Al (CG Al). In another study conducted by Ye *et al.* [13], the compressive strength of Al5083-B₄C trimodal composite has been reported up to 1000 MPa, i.e. three times of the compressive strength of 5083 alloy. Most of the studies conducted on bimodal aluminum alloy are about 5083 Al alloy. However, little research has been done on bimodal 2024 Al alloy. So, the microstructures of this tri-modal composite have been investigated and the structure-properties relationships are explored in the present study.

2. Experimental

Al2024 powder, atomized by Argon gas, with a mean size of 60 μm, was used as matrix. B₄C powder with a mean particle size of 20 μm in 5 wt% was also used as reinforcement.

An attrition mill equipped with water cooling system was used for mechanical milling process and producing Al2024-5wt%B₄C composite powder (NC Al-B₄C sample). Ball-to-powder weight ratio and the rotational speed were defined 1:10 and 400 rpm, respectively. After the mechanical milling, the hot extrusion process was used for the final forming of powders. The powders were hot pressed into a cylinder mold at 100°C. Then, the hot pressed powders were exposed to hot extrusion in 570°C with extrusion ratio of 10:1 without atmospheric control and left to cool under ambient conditions to room temperature. The final product consisted of cylindrical bars with a diameter of 10 mm. To study the effect of B₄C particles and mechanical milling on Al2024 alloy properties, a coarse-grain sample (CG Al) using unmilled Al2024 powder was produced through hot-pressing and then hot extrusion. For the trimodal composites, 2 batches of MMC samples were fabricated via mixing the Al-B₄C milled powder with 30 wt% and 50 wt% of coarse grained aluminum particles, respectively, designated as Al-B₄C 30-70 and Al-B₄C 50-50. To mix the milled powders with coarse-grained aluminum powder a low-energy ball mill was used. The mixed powders were then exposed to hot extrusion at 570°C.

Microstructural characterizations of hot extruded samples were carried out using the

optical microscopy, Transmission electron microscopy (Philips FEQC200) and Scanning electron microscopy (TESCAN XMU VEGA-II) equipped with EDS spectroscopy. The grain size and lattice strain of samples before and after hot extrusion were investigated using Clemex image analyzer and Williamson–Hall method [14]. To compare the mechanical properties of samples, tension, compression and hardness tests were applied. The samples of tensile test were provided according to ASTM B557 and the test was performed at room temperature at displacement rate of 1 mm/min. To determine the fracture mode of samples, the fracture surface was examined by SEM after tensile test. The compression test was also performed according to ASTM E9 at room temperature at displacement rate of 1 mm/min. The samples of compression test were produced with 1/4 aspect ratio. All compression specimen surfaces were polished using a high-grade abrasive paper to provide a

uniform surface roughness. The graphite powder was used as a lubricant to reduce the friction during the deformation compression tests. The hardness of samples was measured by Brinell hardness test with ball diameter of 2.5 mm and 30 kg force.

3. Results and Discussion

X-ray diffraction patterns of unmilled (CG Al) and mechanically milled (NC Al-B₄C) powders are shown in Figure-1. As seen in this figure, after addition of boron carbide particles and 50 h mechanical milling, peaks are broadened and peak heights are decreased, as a result of grain refinement and an increase in internal strain due to mechanical milling. To determine the lattice strain and powder grain size Williamson–Hall equation was employed. As expected, SPD of powder particles during mechanical milling process reduced the size of aluminum matrix grains <100 nm (Table 1).

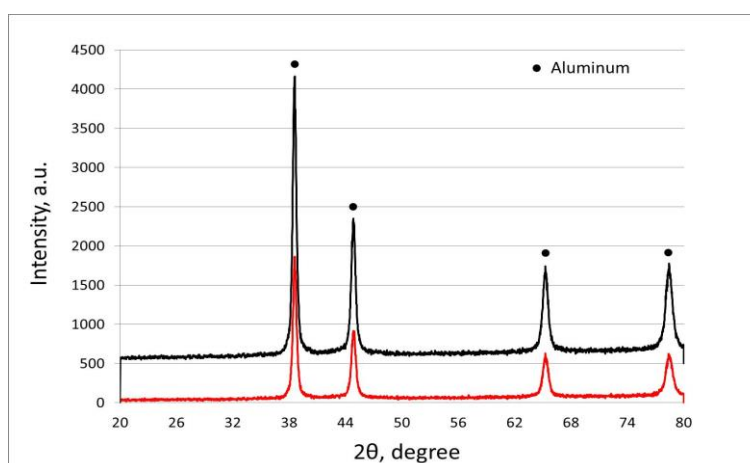


Fig.1. X-ray diffraction patterns of unmilled (CG Al) and mechanically milled (NC Al-B₄C) powders

Table 1. Grain size and lattice strain of powder samples (before extrusion)

Sample name	Grain size (nm)	Lattice strain (%)	Calculation method
CG Al	107	0.012	Williamson–Hall
NC Al-B ₄ C	31	0.026	Williamson–Hall

Figure 2 shows BF-TEM image of NC Al-B₄C sample with nano-sized grains. In the previous study [8] the authors proved that SPD powder particles during mechanical milling decreases the crystal size of matrix to nanometer, so that matrix grain size decrease to <100 nm.

Figure 3 shows optical micrograph of CG Al and NC Al-B₄C samples in parallel and perpendicular to the extrusion direction. This figure shows that the grain size decreases severely after mechanical milling process so that the grain boundaries are not visible in the microstructure of NC Al-B₄C sample.

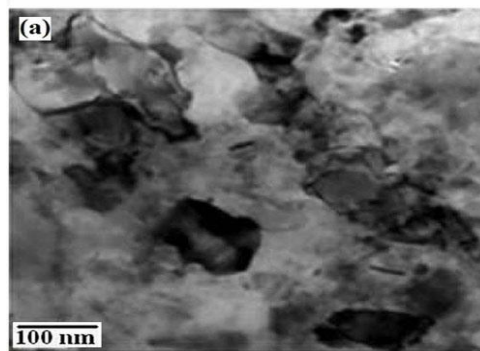


Fig. 2. BF-TEM micrograph of NC Al-B₄C sample after hot extrusion

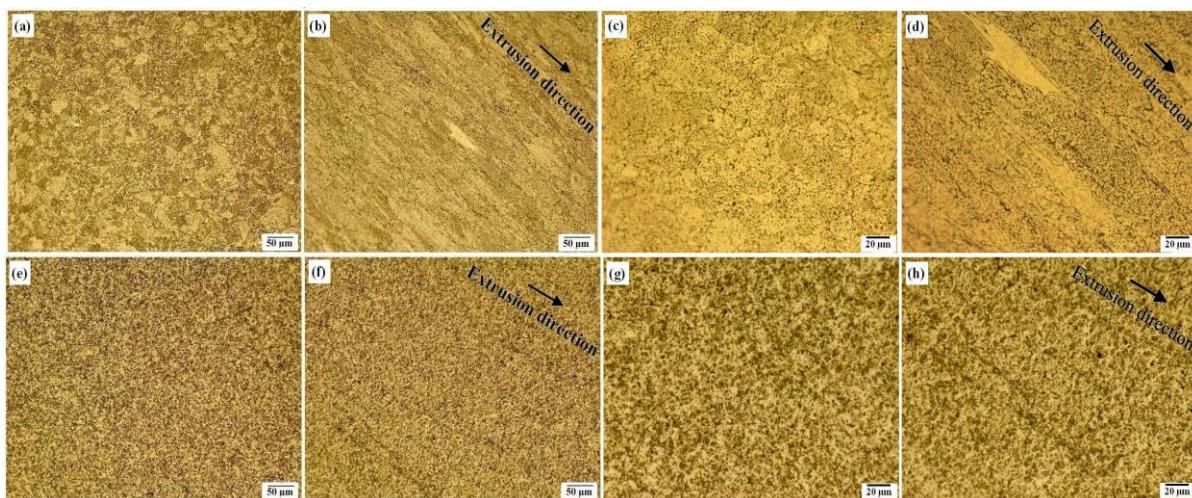


Fig. 3. Optical micrographs of NC Al (a-d) and NC Al-B₄C (e-h) samples in parallel and perpendicular to the extrusion direction

Figure 4 shows optical micrograph of Al-B₄C 50-50 and Al B₄C 30-70 trimodal composites parallel and perpendicular to the extrusion direction. The microstructure

consists of light areas surrounded by dark areas. In this figure, light areas refer to coarse-grained aluminum (CG Al) and dark areas refer to nano-structured aluminum (NC Al).

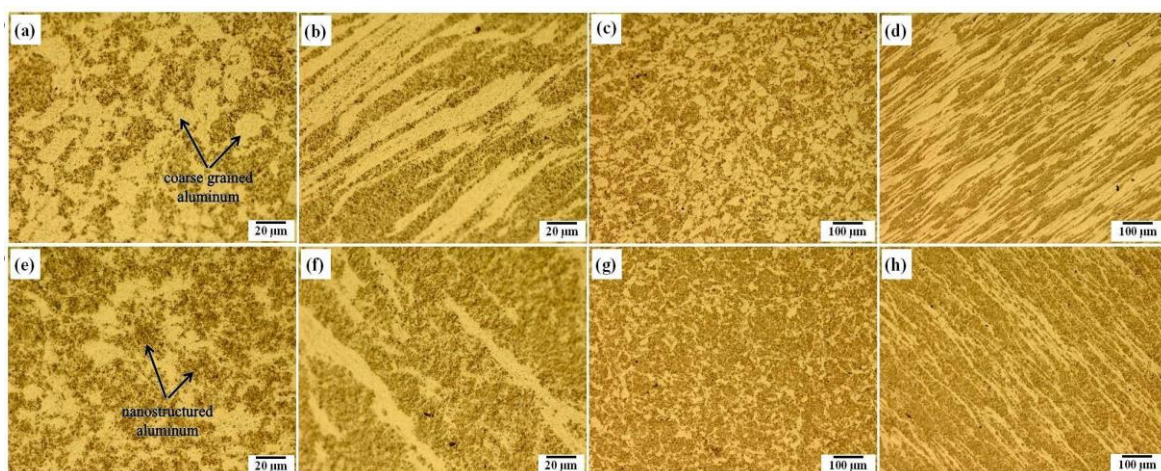


Figure 4. Optical micrographs of trimodal composites: Al-B₄C 50-50 (a-d) and Al-B₄C 30-70 (e-h) parallel and perpendicular to the extrusion direction

As shown in Figure 4, coarse-grained aluminum particles are along the extrusion direction and surrounded by nanostructured regions. Uniform distribution of coarse-grained particles is one of the most important results that can be observed in the microstructure of trimodal samples. The increase in coarse-grained aluminum fraction reduces the distance between CG Al bands and in some areas; these bands are attached to each other. Moreover, the length and thickness of CG Al bands has increased (the aspect ratio has increased), i.e., in Al-B₄C 30–70 samples, containing a lower percentage of coarse-grained aluminum particles, CG Al bands are shorter and narrower (the aspect ratio is less).

The orientation of B₄C containing milled phase and matrix grains along the extrusion direction is evident in the microstructure of samples. The shear stress, occurred during extrusion process, leads to the decrease of porosity in particle/matrix interphase that results in the bonding of particles and matrix phase improves. As a result of this shear stress, the B₄C containing milled phase orient in the direction that would have been under less stress. Therefore, as showed in Figures-3 and 4, B₄C containing milled phase and grain matrix would be orientated along the extrusion direction.

Figure 5 shows SEM micrograph of samples in parallel and perpendicular to the extrusion direction. In this figure, the results of EDS analysis are included that shows that dark points refer to B₄C particles. White points in SEM images are Cu rich phases. These phases are probably Al₂CuMg intermetallic compound [15-17] which are formed and precipitated because Al2024 is first exposed to high temperature (during extrusion process) and then cooled in the air (after extrusion die exit). These compounds which are called S' precipitates [16] are formed during age-hardening heat treatment (precipitation hardening). In other words, matrix alloy, because of being exposed to high temperature (570^oC) during extrusion process and then being cooled to room temperature (in the air), has been age hardened (or precipitation hardened) [16]. Similar observations were previously made by Abd El-Azim *et al.* [18] for Al2024-Al₂O₃

composites. In the research study of age-hardening kinetics, it has been shown that the addition of ceramic particles to age-hardenable Al alloys has different effects on precipitation of composite compared with unreinforced alloy [19]. When a particular reinforcement is introduced into a heat-treatable aluminum alloy matrix, similar aging characteristics might be expected for both composite and unreinforced material. The kinetics of aging can also be different, and both enhanced and retarded behavior has been exhibited in different MMC systems [20]. It was proposed that the addition of reinforcing particles accelerates the aging kinetics [19]. Thomas and King [21] stated that in Al2124 based composites, the presence of reinforcing particles facilitates the nucleation of S' that results in the reduction of the required time to achieve peak hardness.

An accelerated aging phenomenon has been reported for the Al6061-B₄C particulate composite in comparison with an unreinforced matrix alloy. This acceleration was attributed to a decrease in the incubation time required for the nucleation event and a concomitant increase in the solute diffusivity, and therefore in the rate of precipitate growth [20].

The precipitation sequence of the composite was similar to that of the unreinforced alloy, but the aging kinetics was altered. Aging was accelerated because solute diffusivity increased as dislocation density also increased [22]. The distribution of precipitation particles (S') determines the quality of mechanical properties [23]. The result of element mapping (Fig. 5) reveals that these phases are distributed uniformly throughout the matrix alloy that leads to increase in mechanical properties.

As shown in SEM image of samples, B₄C particles are distributed uniformly throughout the matrix and no clustering or agglomeration is observed. Considering the microstructure of trimodal composites, microstructural uniformity occurs in two different levels: 1. Uniform distribution of CG Al particles; 2. Uniform distribution of B₄C particles in NC Al regions. As shown in Figure 5, structural uniformity has occurred on both levels for trimodal composites. The distribution uniformity of B₄C particles occurs during

mechanical milling; however, distribution uniformity of CG Al particles occurs in low-energy ball mill (mixing process of CG Al and

NC Al powders). This distribution uniformity in two different levels improves samples mechanical properties.

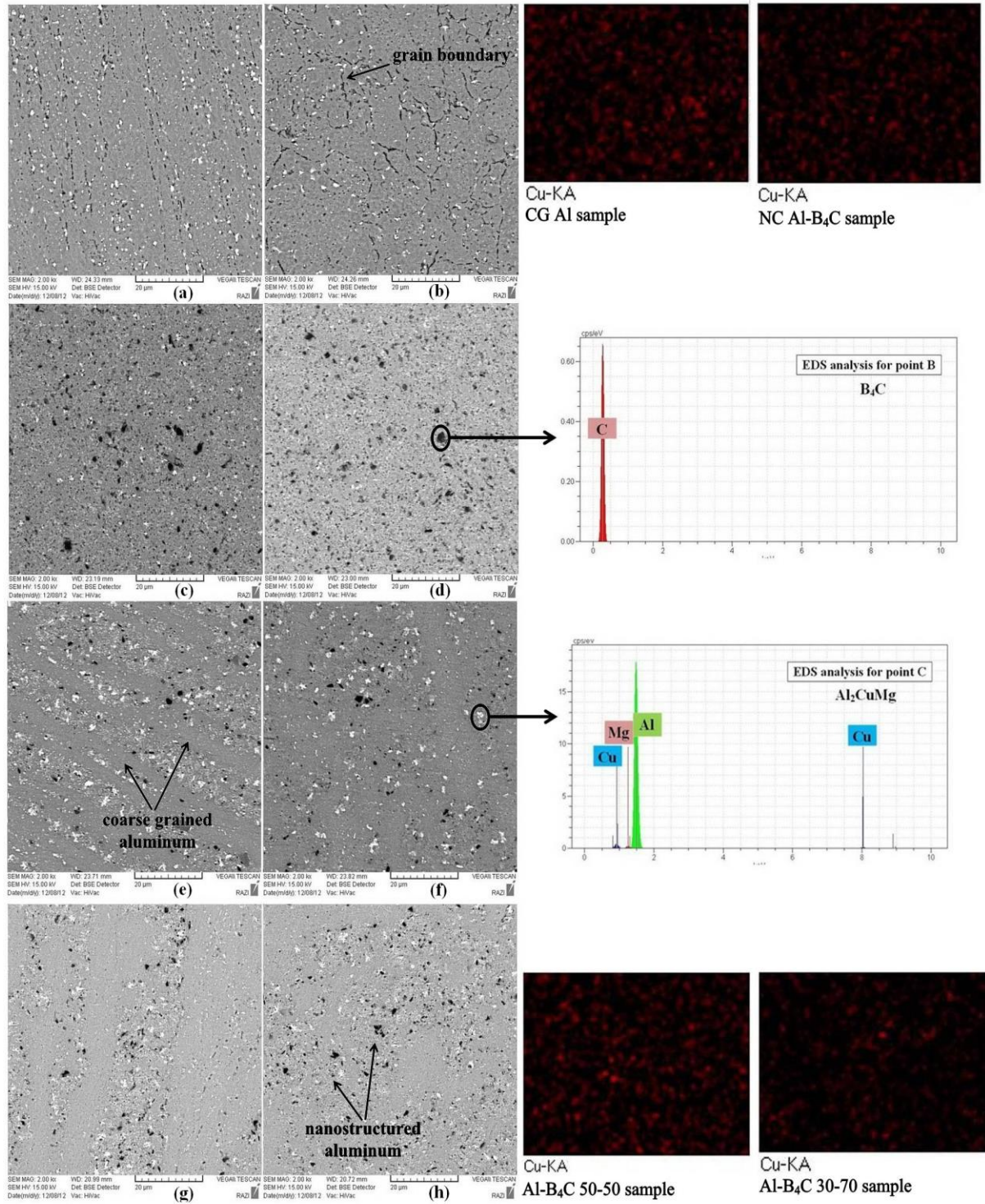


Fig. 5. SEM images and element mappings of: CG Al (a,b); NC Al-B₄C (c,d); Al-B₄C 50-50 (e,f) and Al-B₄C 30-70 (g,h) parallel and perpendicular to the extrusion direction

The engineering stress-strain curves of samples are also compared with each other in Figure 6. The NC Al-B₄C sample has the highest strength (582 MPa) and lowest elongation (0.5%). In contrast, CG Al sample has the highest elongation (14.4%) and lowest strength (340 MPa).

The changes in yield strength and tensile strength of hot extruded samples could be explained by Hall-Petch mechanism and Orowan mechanism. According to Hall-Petch mechanism, the yield stress is inversely related to the grain size; therefore, by reducing the

grain size, the yield strength increases [24]. Since mechanical milling process causes grain refinement (Table 2), according to Hall-Petch mechanism, the yield stress NC Al-B₄C sample would be higher than of CG Al sample. A physical basis for this behavior is associated with the difficulty for dislocations to move across grain boundaries and the associated stress concentrations due to dislocation pile-up [25]. Han *et al.* [26] in their research on Al5083 alloy proved that mechanical milling enhances the strength of alloy up to 713 MPa but reduces its ductility to 0.3%.

Table 2. Grain size of samples after hot extrusion

Sample	Grain size	Calculation method
CG Al	8 (μm)	Clemex image analyzer
NC Al-B ₄ C	100 (nm)	Williamson-Hall

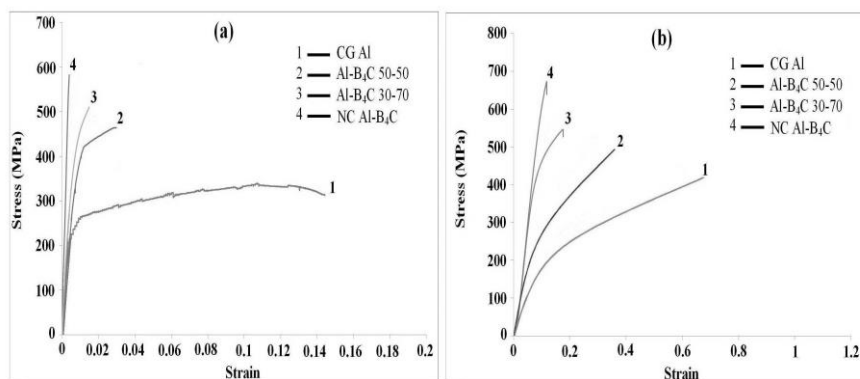


Fig. 6. a) Tensile, and b) Compression Engineering stress-strain curves of hot extruded samples

The effect of B₄C particles on NC Al-B₄C sample strength increase could be explained by Orowan strengthening mechanism [8]. According to this mechanism, by adding reinforcement particles to the matrix, the obstacles to dislocations movement increase. Therefore, stress required for dislocations (τ) passing through obstacles (particles) increases and as a result the strength enhances.

Figure 7 shows the effect of coarse-grained aluminum particles on tensile strength, yield strength, compressive strength, elongation and hardness of samples. It is clear that as coarse-grained aluminum weight percent increases, the strength decreases but the elongation increases. Hall-Petch and Orowan mechanisms

also apply here. Generally, the strength changes of trimodal composites are attributed to their microstructural characteristics include:

1. weight percent (volumetric percent) of each phases;
2. matrix grain size in CG Al and NC Al areas (Hall-Petch mechanism);
3. reinforcement particles size and their distribution in NC Al areas (Orowan mechanism);
4. distribution of CG Al particles;
5. dislocations density in CG Al and NC Al areas;
6. the quality of interphase between CG Al and NC Al areas [3,13].

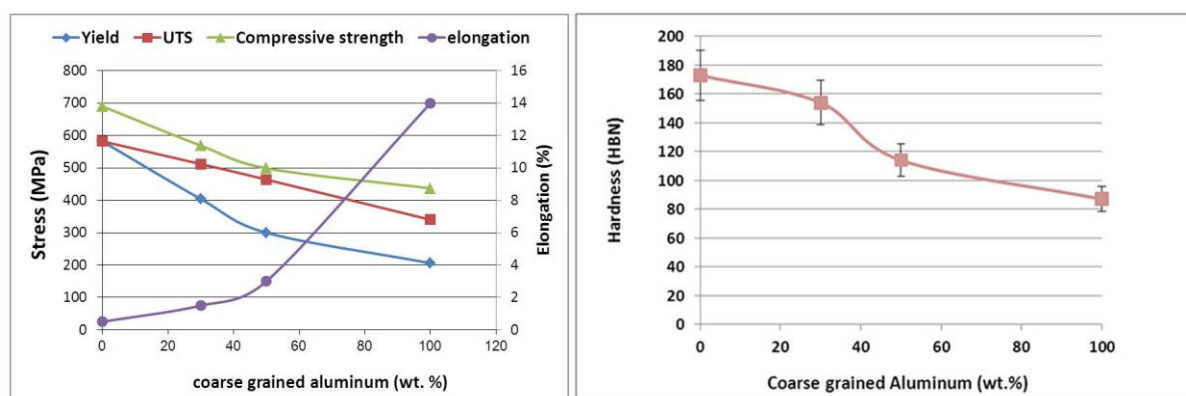


Fig.7. effect of coarse-grained aluminum particles on tensile strength, yield strength, compressive strength, elongation and hardness of hot extruded samples

As the interphase between NC Al and CG Al regions has a good quality (due to the same chemical composition in both the regions), much of the load applied to the sample, transfers from CG Al to NC Al areas and then to B_4C particles, and only a small part remains in CG Al areas. Since this stress is not sufficient for deformation of CG Al regions, the load transformation increases the strength of composite. Therefore, the composite has the ability to tolerate higher level of stress. In summary, it could be said that much of the load applied to the sample is tolerated by NC Al regions and B_4C particles [13, 26].

The increase in tensile strength of samples is inversely related to ductility (elongation), i.e., the increase in strength reduces ductility. Accordingly, NC Al- B_4C sample has the highest level of strength and lowest level of ductility. Since ductility and deformation are strongly dependent on dislocation movement within the sample, another reason that can be offered to explain the low elongation of NC Al- B_4C sample is that in this composite, because of boron carbide particles presence, there are more obstacles to dislocation movements; hence dislocations move difficultly and as a result the elongation or ductility decrease [27]. Moreover, SPD applied on powder particles during mechanical milling, reduces matrix grain size. Following matrix grain size reduction, the grain boundaries density increases remarkably, and since grain boundaries is an obstacle to dislocation movement, as grain boundaries increases, the dislocation movements and ductility decrease. This could be explained by

Orowan relationship [24]. The more obstacles to dislocation (reinforcing particles or grain boundaries) movement are, the mean distance moved by dislocations reduces and the strain imposed on the sample reduces as well [7].

As shown in Figure 7, as coarse-grained aluminum weight percent increases, the strength decreases and the elongation increases. The reason is that, when load is applied, deformation first begins in NC Al regions and expands, but before this regions experiences fracture, the load transformation mechanism is activated and the tensile stress transfers from NC Al to CG Al regions, where experience plastic deformation under lower stress. This causes a slight reduction in the strength trimodal composites, but their ductility increase in return. On the other hand, because of CG Al particles presence, the number of obstacles to dislocations movement is smaller and the mean distance moved by dislocation is greater. Therefore, according to Orowan mechanism the sample tolerates greater strain and its ductility increases. Given the above, it is clear that as coarse-grained aluminum weight percent increases, the strength decreases slightly but the ductility increases [7]. However, this seems inconsistent with the theory of Ye *et al.* [13]. As mentioned in the previous section, Ye *et al.* used load transformation mechanism from CG Al to NC Al areas to explain the strength of trimodal composites; but here the load transformation mechanism has occurred from NC Al to CG Al areas. To explain this contradiction, it can be said that if CG Al phase value is over 50%, it will act as matrix

phase. Therefore, the load transfers from CG Al (matrix phase) to NC Al regions (reinforcing phase). However, if CG Al phase value is <50%, unlike the previous condition, NC Al phase (which is greater) acts as matrix phase and therefore, the load transfers from NC Al (matrix phase) to CG Al regions (reinforcing phase).

The mechanism reported to increase the strength and ductility simultaneously in trimodal composites is related to the microstructure of these composites. It explains that increase in ductility is due to more movement of dislocation in CG Al regions [28, 29] and increase in strength is due to restriction in plastic deformation of CG Al areas by NC Al regions. Because CG Al regions are surrounded tightly by NC Al phase and their plastic deformation decrease severely (NC Al phase prevents plastic deformation in CG Al regions) [29].

Previous works on bimodal aluminum alloys demonstrate that during tensile testing, micro cracks first form in the nanostructured regions because of their relatively high stress

concentration and low ductility [9]. The CG Al phase prevents stress concentration in NC Al and as a result delays crack initiation and growth in these areas [30]. However, if the crack initiates and grows in NC Al regions (when load is applied) as it reaches CG Al particles, it will be impeded or bridged by ductile elongated coarse grains. Hence, CG Al particles could increase ductility through crack impedance/deflection [9].

In summary, it can be said that deformation initiates from NC Al regions. Then the cracks caused by deformation, grow and as they reach CG Al regions are impeded [7]. CG Al particles oriented along extrusion direction act as ductile whiskers and as the crack energy decreases, the ductility of composite increases [13]. The crack initiation and growth in nanostructure regions and crack impedance or deflection as it reaches CG Al regions are shown in fracture surface. Figure-8 shows the fracture surface of trimodal composites. As it can be seen from these images, crack initiates in NC Al regions and impedes, or deflects as it reaches CG Al regions.

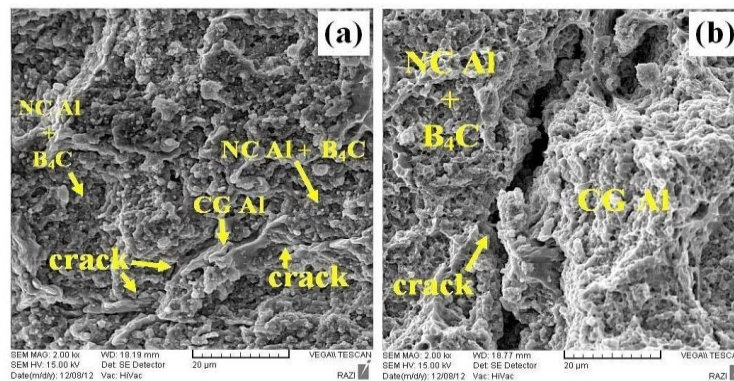


Fig. 8. Increase in ductility of trimodal composites through crack deflection and impedance: (a) Al-B₄C 50-50 and (b) Al-B₄C 30-70

In some cases the weight percent of the coarse grain is very low to block the propagation of all cracks. That is, a critical weight percent of coarse grain exists, above which the micro cracks can be completely prevented by the coarse grains during the plastic deformation. When the weight percent of the coarse grain is less than this threshold, there must be a dominant micro crack that can go around the coarse grains to cross the sample. The probability of such a micro crack

crossing the sample increases with the decrement of the weight percent of the coarse grain (Fig. 9) [31]. Beside, Han *et al.* [10] demonstrated that 30–50% of coarse grains added to a nanostructured matrix could lead to an enhanced ductility with minimum reduction in strength. Therefore, it can be concluded that the main reason for ductility increase in Al 50-50 and Al 30-70 samples is crack impedance/deflection.

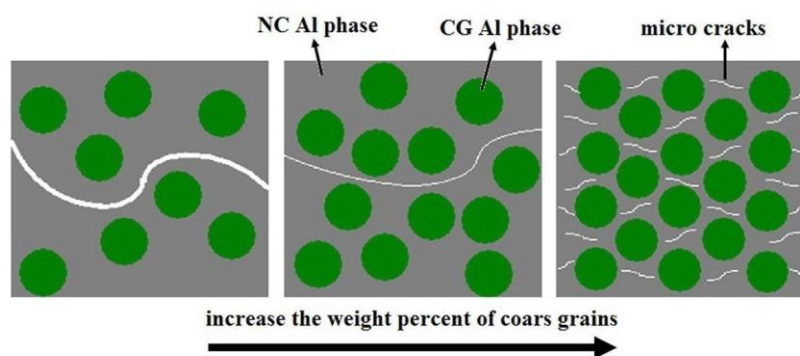


Fig. 9. Schematic image of crack impedance/deflection in bimodal metals/ alloys [31]

The hardness of B_4C is much higher than the hardness of aluminum, the increase in hardness by addition of B_4C is not unexpected. This could be easily analyzed according to mixture rule [27]. Hardness increase due to reinforcing particles addition is attributed to dispersion strengthening (Orowan mechanism). By adding B_4C particles to aluminum matrix, the number of obstacles to dislocations movement increases (their movement is delayed) and the hardness increases as well.

Since the hardness of NC Al- B_4C sample is higher than the hardness of CG Al sample, it can be concluded that in trimodal composites, as the percentage of coarse-grained aluminum increases, the hardness decreases (Fig. 7).

Figure 7 shows the compressive strength of NC Al- B_4C sample is higher than CG Al sample and the reason is grain refining during mechanical milling. That is, Hall-Petch mechanism applies here as well and refined structures show higher compressive strength. The results of tensile test showed in compression test NC Al- B_4C sample in comparison to CG Al sample has a lower ductility and tolerates a slight strain before it fractures (has a low strain-to-failure).

Because of boron carbide particles presence, Orowan strengthening mechanism is activated and helps increase in compressive strength of NC Al- B_4C sample. Meanwhile, boron carbide particles delay crack initiation and growth, particularly, in the early stages of barreling and thereby also increases the compressive strength [27]. What should be noted about compressive strength of trimodal composites is that as coarse-grained aluminum weight percent increases, the compressive strength decreases (Fig. 8), but the sample

tolerates higher strain before it fractures (the ductility increases). Since the results are very similar to the results obtained from tensile test, so the reasons mentioned for the tensile strength increase applies here too.

3.1. Damage and failure behavior

Figure 10 shows the fracture surface of samples after the tensile test. Since the areas of ductile fracture are detected as dimple in images of fracture surface, the more dimples are in fracture surface, the higher the ductility of sample is and ductile fracture occurs. Accordingly, the fracture surface of CG Al sample indicates characteristics of ductile fracture comparing to NC Al- B_4C sample. This happens due to ductile aluminum matrix without hard and brittle B_4C particles. It can be said that dimple nucleation in CG Al sample is concentrated in matrix inclusions and then these dimples growth and join together and finally cause the sample to fracture. This fracture mechanism is called dimple rupture. If there is no inclusion in matrix, dimples nucleate in grain boundaries [32]. In contrast, as seen in Figure 13, the fracture in NC-Al sample has been totally brittle, i.e., it has occurred through brittle-cleavage fracture [25]. These results confirm the reduction of ductility in NC Al- B_4C sample in contrast with CG Al sample.

In the fracture surface of trimodal composites, depending on coarse-grained aluminum weight percent, the characteristics of ductile and brittle fracture are seen simultaneously. Areas, experienced ductile fracture (have more dimples), are related to CG Al phase fracture. But, flat areas which have no dimples indicate brittle fracture in NC

Al regions [13]. That is, in trimodal composites, ductile fracture and brittle fracture occur along CG Al bands and NC Al bands, respectively. Therefore, it is clear that by increasing coarse-grained aluminum weight percent, the fracture mechanism changes from brittle to ductile. These results match the increase in ductility of trimodal composites due to increase in coarse-grained aluminum weight percent.

Stress-strain curves of samples also show that NC Al sample experienced brittle fracture without plastic deformation (or necking), whereas CG Al sample has fractured after tolerating a considerable plastic deformation. That is exactly the reason the yield strength

and ultimate tensile strength (UTS) are equal in NC Al sample. The stress-strain curve of bimodal alloys indicates that as the coarse-grained aluminum weight percent increases, the strain-to-failure (or work-hardening) and the area covered under the curve increase as well. There are many obstacles to dislocations movement in nanostructure material (because the grains are fine). Dislocations move very difficult and the ability to create working-hardening in these materials is very low. These materials do not experience considerable plastic deformation and after passing the yield point, without necking (or plastic deformation) experience a completely brittle fracture [33].

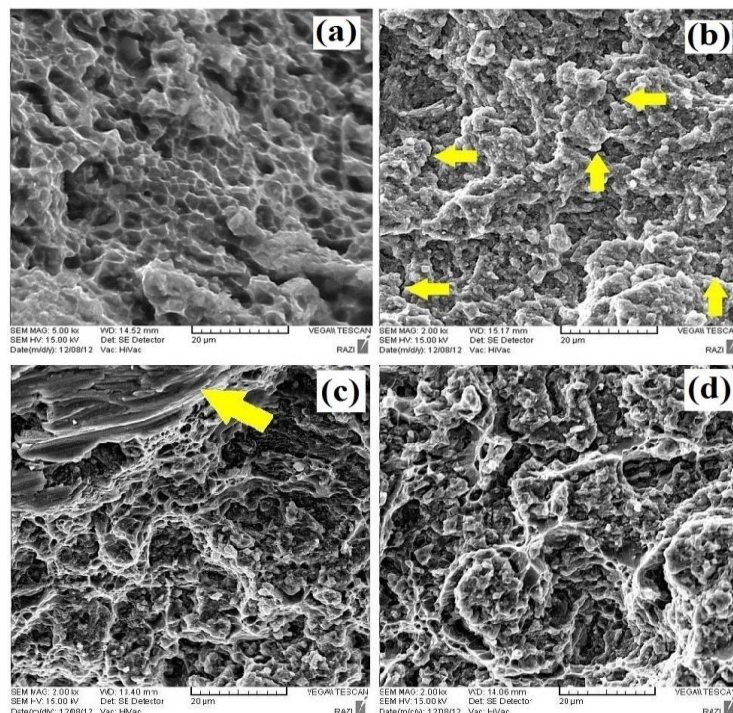


Fig. 10. Fracture surface of the a) CG Al; b) NC Al-B₄C; c) Al-B₄C 50-50 and d) Al-B₄C 30-70 samples

4. Summary and Conclusions

In the present paper, trimodal 2024 Al alloy based composites were produced by mechanical milling and hot extrusion and their mechanical properties were compared with each other. The results show that the strength, after 50 h milling and addition of 5wt% B₄C, increase from 340 to 582 MPa and the hardness increased from 87 HBN to 173 HBN but the elongation decreased from 14 to 0.5%. By adding the coarse-grained aluminum

powder, the strength and hardness decrease slightly, but the ductility increases in return. Ductility increase is a result of increase in dislocation movements and strength increase is a result of restriction in plastic deformation by nanostructured regions. Furthermore, the strength and hardness of trimodal composites were higher but their ductility was lower. The fracture surface of CG Al sample indicates the characteristics of ductile fracture comparing to NC Al-B₄C sample. In trimodal composites,

addition of coarse-grained aluminum from 0 to 100 wt% changes the fracture mechanism gradually from brittle to ductile. In fact, in trimodal composites, ductile fracture and brittle fracture occur along CG Al and NC Al bands respectively. Inspection of the deformation characteristics indicates that the higher ductility in bimodal Al2024 alloys is attributed to the retardation of micro crack nucleation and propagation and crack impedance /deflection by coarse grains.

References

- [1]. Ahn, B., Nutt, S. R., *Exp. Mech.* Vol. 50 (2010) pp.117–23.
- [2]. Lee, Z., Witkin, D. B., Radmilovic, V., Lavernia, E. J., Nutt, S. R., *Mater. Sci. Eng. A* Vol. 410-411 (2005) pp. 462–7.
- [3]. Yao, B., Hofmeister, C., Patterson, T., Sohn, Y., Bergh, M., Delahanty, T., Cho, K., *Composites part A* Vol. 41 (2010) pp. 933–41.
- [4]. Witkin, D., Han, B. Q., Lavernia, E. J., *Metall. Mater. Trans. A* Vol. 37 (2006) pp.185-94.
- [5]. Witkin, D., Han, B. Q., Lavernia, E. J., *J. Mater. Eng. Perf.* Vol. 14 (2005) pp. 519-27.
- [6]. Ahn, J. H., Kim, Y. J., Chung, H., *Rev. Adv. Mater. Sci.* Vol. 18 (2008) pp. 329-34.
- [7]. Witkin, D., Lee, Z., Rodriguez, R., Nutt, S., Lavernia, E. J., *Scripta Mater.* Vol. 49 (2003) pp.297–302.
- [8]. Abdollahi, A., Alizadeh, A., Baharvandi, H. R., *Mater. Design* Vol. 55 (2014) pp. 471–81.
- [9]. Han, B. Q., Huang, J. Y., Zhu, Y. T., Lavernia, E. J., *Acta Mater.* Vol. 54 (2006) pp. 3015–24.
- [10]. Han, B. Q., Lee, Z., Witkin, D., Nutt, S. R., Lavernia, E. J., *Metall. Mater. Trans. A* Vol. 36 (2005) pp. 957-65.
- [11]. Tellkamp, V. L., Dallek, S., Cheng, D., Lavernia, E. J., *J. Mater. Res.* Vol. (2001) pp.938-44.
- [12]. Hofmeister, C., Yao, B., Sohn, Y. H., Delahanty, T., Bergh, M., Cho, K., *J. Mater. Sci.* Vol. 45 (2010) pp. 4871–6.
- [13]. Ye, J., Han, B. Q., Lee, Z., Ahn, B., Nutt, S. R., Schoenung, J. M., *Scripta Mater.* Vol. 53 (2005) pp. 481- 6.
- [14]. Ungar, T., Gubicza, J., Ribarik, G., Borbly, A., *J. Appl. Cryst.* Vol. 34 (2001) pp. 298–310.
- [15]. Porter, P. A., Easterling, K. E., *Phase Transformation in Metals and Alloys* (1981) England: Van Nostrand Reinhold Company.
- [16]. Totten, G. E., MacKenzie, D. S., *Handbook of Aluminum* (2003) New York: Marcel Dekker Inc.
- [17]. Avner, S. H., *Introduction to Physical Metallurgy* (1974) New York: McGraw-Hill.
- [18]. Abdel-Azim, A. N., Shash, Y., Mostafa, S. F., Younan, A., *J. Mater. Proc. Tech.* Vol. 55 (1995) pp. 140–5.
- [19]. Mousavi Abarghouie, S. M. R., Seyed Reihani, S. M., *Mater. Design* Vol. 31 (2010) pp. 2368–74.
- [20]. Bekheet, N. E., Gadelrab, R. M., Salah, M. F., Abd El-Azim, A. N., *Mater. Design* Vol. 23 (2002) pp.153-9.
- [21]. Thomas, M. P., King, J. E., *J. Mater. Sci.* Vol. 29 (1994) pp. 5272–8.
- [22]. Appendino, P., Badini, C., Marino, F., Tomasi, A., *Mater. Sci. Eng. A* Vol. 135 (1991) pp. 275–9.
- [23]. Saha, P. K., *Aluminum Extrusion Technology* (2000) USA: ASM International.
- [24]. Dieter, G. E., *Mechanical Metallurgy* (1986) New York: McGraw-Hill.
- [25]. Alizadeh, A., Taheri-Nassaj, E., *Mater. Charact.* Vol. 67 (2011) pp. 119-28.
- [26]. Han, B.Q., Ye, J., Tang, F., Schoenung, J., Lavernia, E. J., *J. Mater. Sci.* Vol. 42 (2007) pp. 1660–72.
- [27]. Rahimian, M., Parvin, N., Ehsani, N., *Mater. Sci. Eng. A* Vol. 527 (2010) pp. 1031–8.
- [28]. Wang, Z., Song, M., Sun, C., Xiao, D., He, Y., *Mater. Sci. Eng. A* Vol. 527 (2010) pp. 6537–42.
- [29]. Vogt, R. G., Zhang, Z., Topping, T. D., Lavernia, E. J., Schoenung, J. M., *J. Mater. Process. Technol.* Vol. (2009) pp.5046–53.
- [30]. Fan, G. J., Choo, H., Liaw, P. K., Lavernia, E. J., *Acta Mater.* Vol. 54 (2006) pp.1759–66.
- [31]. Zhu, L., Shi, S., Lu, K., Lu, J., *Acta Mater.* Vol. 60 (2012) pp. 5762–72.
- [32]. Kang, Y. C., Chan, S. L. I., *Mater. Chem. Phys.* Vol.85 (2004) pp. 438–43.
- [33]. Cheng, S., Ma, E., Wang, Y. M., Kecskes, L.J., Youssef, K. M., Koch, C. C., Trociewits, U. P., Han, K., *Acta Mater.* Vol. 53 (2005) pp. 1521–33.